



Article

Climate-Smart Agro-Hydrological Model for a Large Scale Rice Irrigation Scheme in Malaysia

Habibu Ismail ^{1,2}, Md Rowshon Kamal ^{1,*}, Ahmad Fikri bin Abdullah ¹ and Mohd Syazwan Faisal bin Mohd ³

¹ Department of Biological and Agricultural Engineering, Faculty of Engineering, Universiti Putra Malaysia, UPM Serdang 43400, Selangor DE, Malaysia; habfta@yahoo.com (H.I.); ahmadfikri@upm.edu.my (A.F.b.A.)

² Department of Agricultural and Bio-Resources Engineering, Ahmadu Bello University, Zaria 810107, Kaduna State, Nigeria

³ Water Resources Research Centre and Climate Change, National Hydraulic Research Institute of Malaysia (NAHRIM), Seri Kembangan 43300, Selangor DE, Malaysia; syazwan@nahrim.gov.my

* Correspondence: rowshon@upm.edu.my; Tel.: +603-9769-4339

Received: 25 March 2020; Accepted: 27 April 2020; Published: 4 June 2020



Abstract: Agro-hydrological water management frameworks help to integrate expected planned management and expedite regulation of water allocation for agricultural production. Low production is not only due to the variability of available water during crop growing seasons, but also poor water management decisions. The Tanjung Karang Rice Irrigation Scheme in Malaysia has yet to model agro-hydrological systems for effective water distribution under climate change impacts. A climate-smart agro-hydrological model was developed using Excel-based Visual Basic for Applications (VBA) for adaptive irrigation and wise water resource management towards water security under new climate change realities. Daily climate variables for baseline (1976–2005) and future (2010–2099) periods were extracted from 10 global climate models (GCMs) under three Representative Concentration Pathway scenarios (RCP4.5, RCP6.0, and RCP8.5). The projected available water for supply to the scheme would noticeably decrease during the dry season. The water demand in the scheme will differ greatly during the months in future dry seasons, and the increase in effective rainfall during the wet season will compensate for the high dry season water demand. No irrigation will therefore be needed in the months of May and June. In order to improve water distribution, simulated flows from the model could be incorporated with appropriate cropping patterns.

Keywords: agro-hydrological model; water management; climate change; big data analysis; irrigated rice

1. Introduction

Water crises are a global issue of significant concern. Water is becoming a scarce resource, not only for agriculture, but also for most sectors in most locations across the globe. This is due to efforts to meet industrial and urbanization demands. Climate change is reported to be the main driver of hydrological variations in catchments [1]. The competition for water has increased in recent years to a stage of physical scarcity [2]. In some areas, the streamflow, which is largely the source of water for irrigation, has decreased in recent decades, and projected water declines threaten the sustainability of downstream areas [3]. Future streamflows are also projected to decrease with the impact of climate change [4–7]. Failure of climate change mitigation and adaptation is among the biggest global risks. Agricultural production will be a significant challenge due to population growth and climate change [8]. Agricultural production is one of the most vulnerable sectors to climate change [9]. Soil water balances, evapotranspiration, physiology, and phenology have been altered due to climate

change, which has consequently affected irrigation water requirements. These effects are more severe for a rice crop that consumes high water [10]. The creative, strategic, and economic advancement of food security development in the context of climate change to achieve sustainable agriculture can reduce such threats [9]. Agriculture, therefore, must be ‘climate-smart’, and agricultural systems must be transformed and reoriented to promote food production under these new climate change realities. Improvements in the effectiveness of agricultural water use could result in sufficient water for domestic use in high-competition watersheds. This potentially represents a significant adaptation approach for global change [11]. The information linked to agro-hydrological procedures is helpful for improving watershed hydrological modeling and agricultural production [12].

Agro-hydrological water management frameworks help to integrate expected planned management and expedite regulation of water allocation for agricultural production. Low production is not only due to the variability of available water during the crop growing seasons, but also due to poor water management decisions, such as not considering the available water for irrigation [13]. A climate-smart agro-hydrological model can be a robust solution for wise water management decisions in a large-scale irrigation scheme to cope with the risk of water and food security under the new realities of climate change. Several approaches have been adopted for the integration and analysis of large input data to improve decision making in agriculture. For instance, a context-aware systems (CAS) was developed to automate a manual irrigation method by integrating two engineering methodologies: ontology and information systems [14]. A climate-smart decision support system (CSDSS) was developed for analyzing the water demand of a large-scale rice irrigation scheme [15]. An agricultural data analysis approach, which can estimate the weight of onions during the growth stages, was introduced using a functional regression model [16]. A seasonal furrow irrigation model was developed using different data sets to estimate and analyze information of every event of furrow irrigation for maize crop production [17]. A process-based regional economic optimization (PBREOP) tool was developed to optimize the irrigation water use efficiency and economic benefit of an irrigation area, which reduced the total amount of irrigation water used by an average of 23% without a reduction in benefits [18]. The PBREOP model is a two-level optimization model with combined use of an agro-hydrological model (SWAP-EPIC). An agro-hydrological model, Soil-Water-Atmosphere-Plant (SWAP) was applied to assess the effects of management of irrigation water on water and salt balances [19]. The study authors found that the adopted water management in the area leads to excessive irrigation and leaching, as well as elevated groundwater salinity. The agro-hydrological SWAP model was applied under deficit irrigation to assess water cycles in an irrigation area. The optimal practices in irrigation management for hydrologic years were obtained and the average percentage of water saving and groundwater recharge under the optimal irrigation schedules were simulated [20]. Similarly, the agro-hydrological SWAP model was applied to address the salinization of soil and deterioration of water quality. The tool effectively predicted water and salt concentrations of soil, and the reduced effectiveness of relative crop output and water use efficiency [21].

Models could be useful in the assessment of impacts of agricultural management and environmental shifts to support sustainable water management in agricultural, at scales ranging from field to catchment [22]. Despite the availability of a number of available tools, there are still limited studies of the coupling of hydrological and crop models to simulate processes within agro-hydrological watersheds [23]. An integrated system is crucial to address the complexity in various agricultural water management phases within the context of the agro-hydrological watershed, particularly with the emerging issue of climate change. Agricultural use of water is based on various variables including climatic circumstances, topography, lithology, soil, management methods, and plant type. Understanding these parameters enables crop water requirements to be estimated and crop management processes to be established. Existing water management methods might not be sufficient to deal with climate change effects on reliable water supplies for irrigation. Spatial and temporal climate variations have affected water availability in different water catchments globally. Notably, the Tanjung Karang Rice Irrigation Scheme in Malaysia often experiences shortages of water due

to unusual spatial and temporal distributions of rainfall. However, the scheme is yet to model agro-hydrological systems for effective water distribution under climate change impacts. To date, the increasing pressure of demand for water remains a challenge for paddy irrigation planning based on projected multi-models climate data series. Irrigation managers need a tool that helps with quick decisions on water management to mitigate the risk of water and food safety. The aim of this study was to develop a climate-smart agro-hydrological model for adaptive irrigation and wise water resource management towards water security under the new realities of climate change.

2. Materials and Methods

2.1. Study Area

The Tanjung Karang Rice Irrigation Scheme (TAKRIS) is located at about latitude $3^{\circ}25'$ to $3^{\circ}45'$ N and longitude $100^{\circ}58'$ to $101^{\circ}15'$ E in the State of Selangor of Malaysia (Figure 1). The scheme has a 19,030 ha command area [15]. The diversion of water for irrigation is from the Bernam River Basin at the Bernam River Headworks (BRH) situated about 130 km upstream from the estuary of the Bernam River, and reaches the scheme through a feeder canal [6,24]. The feeder canal conveys water over a distance of about 14.5 km into the improved Tenggi River, which runs a further 24.5 km into the Tenggi River Headworks (TRH). The main canal runs for a total of 37.9 km with control structures to irrigate eight irrigation compartments in the scheme. The average annual rainfall in the region is about 2000 mm, the mean monthly temperature is 28°C , and mean monthly humidity is 77% [25,26]. Rice is grown twice per year: during the dry or off-season (January–June) and the wet or main season (July–December). To ensure adequate irrigation deliveries to fields and better water management practices, rice cultivation in the area has been staggered into four Irrigation Service Areas (ISAs I, II, III, and IV) from January (ISA I) to June (ISA IV) during the dry season (Table 1). The process is replicated for the wet season from July (ISA I) until October (ISA IV) before the heavy rains start.

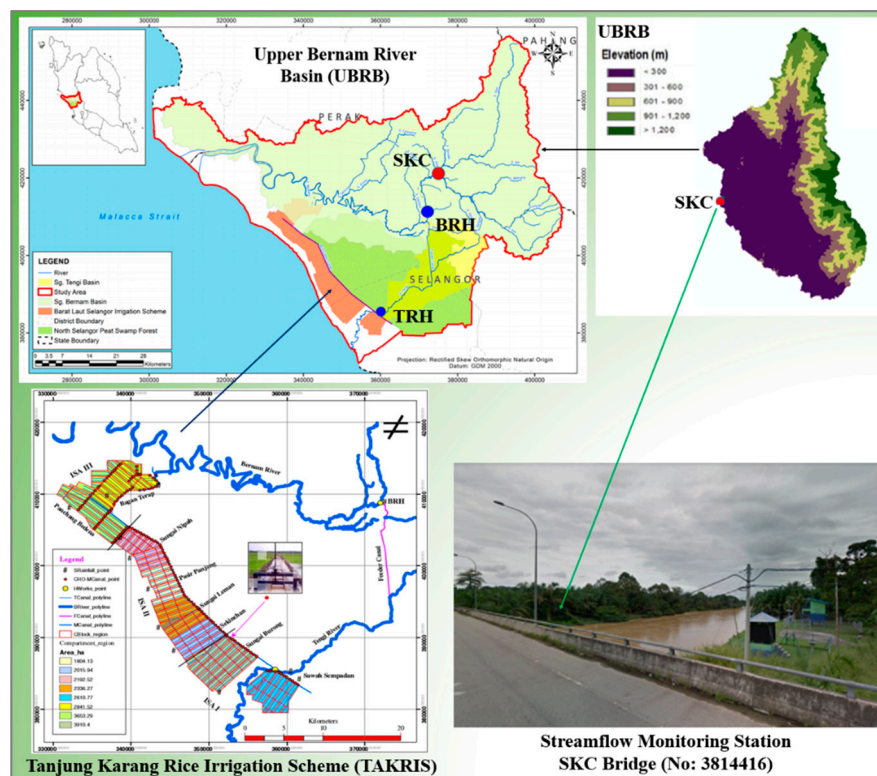


Figure 1. Map of the Tanjung Karang Rice Irrigation Scheme [26].

Table 1. Current cropping calendar and distribution of irrigation supplies for the dry and wet irrigation seasons in the Tanjung Karang Rice Irrigation Scheme.

Cropping Activities	Dry Season				Wet Season			
	ISA I	ISA II	ISA III	ISA IV	ISA I	ISA II	ISA III	ISA IV
Pre-saturation	1-January	1-February	1-March	1-April	1-July	1-August	1-September	1-October
Sowing starts	15-January	15-February	15-March	15-April	15-July	15-August	15-September	15-October
Normal irrigation	1-February	1-March	1-April	1-May	1-August	1-September	1-October	1-November
Irrigation ends	10-April	10-May	10-June	10-July	10-October	10-November	10-December	10-January

2.2. Methodological Approach

The study involves five major aspects related to big data visualization and analysis, namely: (1) extraction and downscaling of daily climate variables to a local station; (2) simulation of climate change impacts on hydrological processes in the Upper Bernam River Basin (UBRB); (3) computation of available discharges for the main water conveyance system from the Bernam River Headwork (BRH) to the Tengi River Headwork (TRH) and at the key points in the main canal; (4) assessment of storage reservoir inflow and release patterns with the need for irrigation water demand and available water for supply under future climate change; and (5) development of a climate-smart agro-hydrological model. Climate variables for baseline (1976–2005) and future (2010–2099) periods were extracted from 10 global climate models (GCMs) under three Representative Concentration Pathway (RCP) scenarios (RCP4.5, RCP6.0, and RCP8.5). The data was downscaled using a developed climate-smart decision support system (CSDSS). The Hydrologic Engineering Center Hydrologic Modeling System (HEC-HMS) hydrological model simulated climate change impacts on hydrological processes in the Upper Bernam River Basin (UBRB) and the Hydrologic Engineering Center River Analysis System (HEC-RAS) hydraulic model was used to compute available discharges for the main water conveyance system from the Bernam River Headwork to Tengi River and at the key points in the main canal. The spatial data required by the models were processed using the GIS extension of the ArcGIS software. Based on design parameters, the inflow and release patterns for a newly built reservoir were assessed with the need for irrigation water demand and available water for supply under future climate change. A climate-smart agro-hydrological model was finally developed using Excel-based Visual Basic for Applications (VBA) to visualize and analyze climate and hydrological knowledge for wise adaptive water management practices under new climate change realities. The systematic approach of the study is depicted in Figure 2.

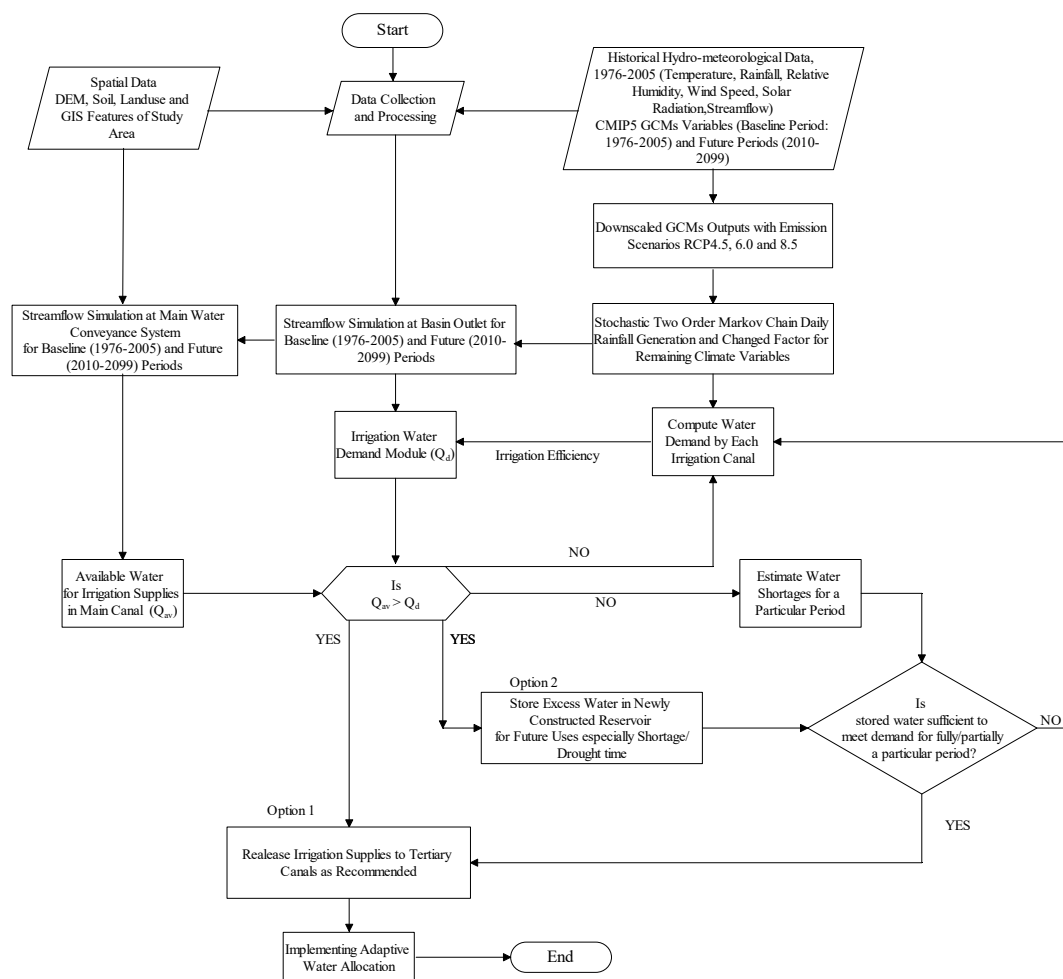


Figure 2. Framework for the development of the climate-smart agro-hydrological model.

2.3. Downscaling of GCMs Outputs

Adoption of multiple models is essential and recommended for impact studies and adaptation strategies [27,28], because a single GCM usually provides uncertain information in assessing the climate change impacts. Therefore, 10 global climate projections were acquired from the Program for Climate Model Diagnosis and Inter-comparison (PCMDI). A baseline period (1976–2005) was adopted and three future periods of 30-year time segments were defined as the 2020s (2010–2039), 2050s (2040–2069), and 2080s (2070–2099) under three RCP scenarios (RCP4.5, RCP6.0, and RCP8.5). The spatial resolution from the output of GCMs cannot provide a suitable climate change scenario for a target watershed because GCMs operate at a larger spatial scale. Therefore, downscaling is required to represent the impact of climate change on a catchment area. A developed CSDSS for downscaling hydro-meteorological variables [15] was adopted to downscale the extracted GCM outputs. The CSDSS was built in the MATLAB environment using the “delta change factor” statistical downscaling method. This method has been widely applied in hydrological modeling because it allows speed of application and direct scaling of the scenarios with respect to changes suggested by the GCMs; moreover, multiple models could be used with the results from various GCM scenarios [29,30]. In the delta change factor method, high resolution future variables at the station scale were created by an ordinary bias correction. Three stations with reliable climate data across the study area were used. The algorithm modifies the observed daily time series of the climate variables by adding and/or

multiplying monthly mean changes of GCM outputs using adjustment formulas. The mean values of GCM simulated baseline and future climates were estimated as:

$$\overline{GCM}_b = \sum_{i=1}^{N_b} GCM_{bi} / N_b, \quad (1)$$

$$\overline{GCM}_f = \sum_{i=1}^{N_f} GCM_{fi} / N_f, \quad (2)$$

where, \overline{GCM}_b and \overline{GCM}_f , GCM_b , and GCM_f are the mean values and values from the GCM baseline and future climate scenario, respectively. N_b and N_f are the total number of values in the downscaling for baseline and future periods, respectively.

Subsequently, monthly additive (CF_{add}) and multiplicative (CF_{mul}) change factors for the baseline and future periods in the equivalent climate variable of interest were calculated for the GCM grid box using Equations (3) and (4). Relative change factors were used in the case of rainfall (ΔP), derived from the ratio of projected-to-baseline averages, while absolute change factors were used for temperature, relative humidity, solar radiation, and wind speed (ΔT), by subtracting the GCM averages representing the baseline from the future.

$$CF_{Rain} = \left(\frac{\overline{P}_{GCM,fut,m}}{\overline{P}_{GCM,base,m}} \right), \quad (3)$$

$$CF_{Temp} = (\overline{T}_{GCM,fut,m} - \overline{T}_{GCM,base,m}), \quad (4)$$

Finally, local-scaled future climate values were obtained by applying the change factors using Equations (5) and (6). This involves superimposing the change factors suggested by the GCM-scenario combinations to the daily baseline time series to yield perturbed climate series.

$$P_{adj,fut,d} = P_{obs,d} \times CF_{Rain}, \quad (5)$$

$$T_{fut,d} = T_{obs,d} + CF_{Temp}, \quad (6)$$

where P and T are the rainfall and climatic variables, respectively; the subscript adj,fut,d denotes the downscaled future daily variable; obs,d denotes daily observations; CF denotes calculated additive and multiplicative change factors for rainfall and climatic variables; and $GCM_{fut,m}$ and $GCM_{base,m}$ are the average monthly values of GCM output and baseline periods, respectively.

A simulation dialog window appears after clicking on a specific command button from the CSDSS main dialog window to generate daily sequences of hydro-meteorological variables. The program was calibrated and validated using the observed and simulated monthly average values for the baseline period. The outputs can be generated as daily time series and long-term monthly time scale, and can be viewed via the “Analysis and Statistics” button as tables and graphs.

2.4. Simulation of Future Impacts of Climate Change on Hydrological Processes

HEC-HMS 4.2.1 was used for simulating precipitation-runoff processes of the UBRB. The model requires two types of data: spatial and hydro-climatic data. The spatial data include a digital elevation model (DEM) downloaded from the Geographic information system software program (DIVA-GIS) website, and soil and land use maps of the area obtained from the Department of Agriculture (DOA) Malaysia. The Arc-Hydro tool coupled with ArcGIS was used to process the spatial data. Due to missing values for a number of years, the observed hydro-climatic data in the area is not reliable. Therefore, a gridded daily dataset including rainfall, minimum and maximum temperature, relative humidity, wind speed, and solar radiation for 1976–2005 was used. The gridded data was at a spatial resolution of 5 km based on the angular distance weighting (ADW) procedure, and covered the entire Peninsular Malaysia [31]. Details of the procedure of data processing and development can be found in other studies [31,32]. The final data used was obtained from the Water Resources and Hydrology Division,

Department of Irrigation and Drainage (DID), Malaysia. Daily discharge records (m^3/s) of the Bernam watershed were taken at gauging station known as SKC.

The HEC-HMS model components include basin model, meteorological model, control specifications, and input data. The components were used to simulate the hydrologic response in the Bernam watershed. The spatial data collected was used to set up the basin model using the GIS component of the model (HEC-GeoHMS), to calculate parameters, such as sub-basin areas, times of concentration, lag time, and reach lengths based on the DEM geospatial information. Subsequently, deficit and constant loss (DCL), simple canopy, and simple surface methods were used for the computation of runoff-volume (loss), canopy, and surface methods, respectively. The Soil Conservation Service (SCS) unit hydrograph (SCS-UH) and constant monthly methods were used for transformation of precipitation excess into point runoff and simulation of time variations in baseflow, respectively. Moreover, for the channel flow, the Muskingum routing method was used as widely adopted by many studies [33,34]. Historical streamflow data for 18 years (1981–1998) was used for model calibration and 8 years (1999–2006) for validation with 5 years of warm up period in each. Manual and automatic calibration techniques were applied to optimize model parameters. The perturbed future rainfall and climate data were used as input variables for the validated HEC-HMS model for modeling future streamflow scenarios of the basin (at the SKC outlet). The validated model was re-run with the downscaled climatic variables for the baseline and the future periods. Consequently, changes to streamflow were analyzed with respect to presently observed and projected future impacts of global climate change.

2.5. Computation of Available Discharges for Irrigation Supply

The HEC-RAS model, which is a computer program that models the hydraulics of water flow through natural rivers and other channels, was adopted in the present study. HEC-RAS 5.0 with the Geospatial Hydrologic Modeling extension (Arc-Hydro and HEC-GeoRAS) was used. Prior to using the model, a DEM raster of the study area was downloaded from DIVA-GIS, and converted to a triangular irregular network (TIN) within Arc-GIS. The TIN was used to establish the river system connectivity, cross section data, reach length, etc., using HEC-GeoRAS. The overall cross section traits of channels were extracted and finally exported into the HEC-RAS model. The earlier simulated streamflow at the SKC by the HEC-HMS model was used as the input hydrograph to the HEC-RAS model for flow routing in the river.

HEC-RAS software is capable of performing one-dimensional (1-D) steady- and unsteady-flow simulations. The unsteady, gradually varied flow simulation model is dependent on finite difference solutions of the Saint-Venant equations as presented in Equations (7) and (8) [35]:

$$\frac{\partial A}{\partial t} + \frac{\partial Q}{\partial x} = 0, \quad (7)$$

$$\frac{\partial Q}{\partial t} + \frac{\partial \left(\frac{Q^2}{A} \right)}{\partial x} + gA \frac{\partial H}{\partial x} + gA(S_o - S_f) = 0, \quad (8)$$

where A = cross-sectional area normal to the flow (m^2); Q = discharge (m^3/s); g = acceleration due to gravity (m/s^2); H = elevation of the water surface above a specified datum, also called stage (m); S_o = bed slope (%); S_f = energy slope (%); t = temporal coordinate; and x = longitudinal coordinate.

The most sensitive calibration parameter required by the HEC-RAS model is channel resistance, specifically, Manning's n . Its values can be extracted with the aid of a land use map of the area using HEC-GeoRAS. However, due to insufficient land use data, covering all of the river area, n values presented by another study [36] were used as a first estimate of the appropriate channel resistance and adjusted through calibration. Because of irregular and limited flow data for the downstream side, located at the inlet of the main canal, reliable data for four years (from 2001 to 2004) were used for model evaluation. The model was calibrated by comparing between the simulated and observed

values using the 2001–2003 daily discharge records of the river. Finally, the calibrated model was validated using the 2004 daily discharge records.

2.6. Statistical Evaluation of Models

The performance of the models was evaluated by comparing the observed discharge with the simulated data using the most commonly used statistical indices as:

- (i) Coefficient of determination, R^2 :

$$R^2 = \left(\frac{\sum_{i=1}^n (P_i^{\text{obs}} - P_i^{\text{mean}})(P_i^{\text{sim}} - P_i^{\text{mean}})}{\left[\sum_{i=1}^n (P_i^{\text{obs}} - P_i^{\text{mean}})^2 \sum_{i=1}^n (P_i^{\text{sim}} - P_i^{\text{mean}})^2 \right]^{0.5}} \right)^2, \quad (9)$$

- (ii) Nash–Sutcliffe efficiency (NSE):

$$\text{NSE} = 1 - \frac{\sum_{i=1}^n (Q_{O_i} - Q_{S_i})^2}{\sum_{i=1}^n (Q_{O_i} - \bar{Q}_O)^2}, \quad (10)$$

- (iii) Percentage bias (PBIAS):

$$\text{PBIAS} = \frac{\sum_{i=1}^N (Q_{O_i} - Q_{S_i})}{\sum_{i=1}^N Q_{O_i}} \times 100\%, \quad (11)$$

2.7. Water Demand Estimation

Several parameters are required to estimate paddy water demands under climate change scenarios. These include the historical and GCM-projected daily hydro-meteorological data, which are needed for estimating reference evapotranspiration, and irrigation requirements of paddy fields and effective rainfall, which need to be estimated using a water balance model. Other related data are crop coefficient, seepage-percolation rate, water application and conveyance losses, and irrigation command area. The daily water demand for the command area was calculated as:

$$\text{IR}_t = \begin{cases} (\text{ET}_{c,t} - \text{ER}_t + \text{SP}_t + \text{RP}_t) & \text{if } \text{RP}_t \leq \text{WD}_{\text{max}} \\ 0, & \text{if } \text{RP}_t > \text{WD}_{\text{max}} \end{cases} \quad (12)$$

where IR_t is the irrigation requirement of the rice crop on the t -th day (mm/day); $\text{ET}_{c,t}$ is the water requirement by the rice crop on t -th day (mm/day); ER_t is the effective rainfall on the t -th day (mm/day); and SP_t is the seepage and percolation losses in a rice field (mm/day). A WD_{max} of 100 mm is usually the standard practice during the normal irrigation supply in Malaysia; however, it varies from 50 mm to 100 mm during irrigation supply periods. RP_t is the required ponding water depth on the day.

A reference evapotranspiration (ET_0)-crop factor (K_c) approach was used to determine the crop requirement ET_c (mm day^{-1}) as expressed in Equation (12). The K_c values for a Malaysian rice variety were used [37].

$$\text{ET}_c = \text{ET}_0 \times K_c \quad (13)$$

The ET_0 (mm day^{-1}) was determined using the FAO-56 Penman–Monteith (PM) model [38]:

$$\text{ET}_0 = \frac{0.408\Delta(R_n - G) + \gamma \frac{900}{T+273} u_2 (e_s - e_a)}{\Delta + \gamma(1 + 0.34u_2)} \quad (14)$$

where ET_o is standardized reference crop evapotranspiration for short grass (mm d^{-1}); R_n is net radiation at crop surface ($\text{MJ m}^{-2} \text{ day}^{-1}$); G is soil heat flux density ($\text{MJ m}^{-2} \text{ day}^{-1}$); T is air temperature at 2 m height ($^{\circ}\text{C}$); u_2 is wind speed at 2 m height (m s^{-1}); $e_s - e_a$ is saturation vapor pressure deficit (kPa); Δ is the slope vapor pressure curve ($\text{kPa } ^{\circ}\text{C}^{-1}$); γ is a psychrometric constant ($\text{kPa } ^{\circ}\text{C}^{-1}$); and 900 is a constant factor.

The projected climate parameters, extracted and downscaled from 10 different GCMs based on three RCP scenarios, were used as basic inputs in the reference ET model for calculating future ET_o series for the period to 2099. Effective rainfall (ER) was derived from the projected rainfall (RF) based on GCM and RCP scenarios. It was calculated based on 1 in 5-year rainfall analysis using the FAO method as:

$$ER = \begin{cases} 0.6RF, & \text{for } RF < 200 \text{ mm/month} \\ 0.3(RF + 200), & \text{for } RF > 200 \text{ mm/month} \end{cases} \quad (15)$$

In this study, average seepage and percolation rates between 2–3 mm/day were adopted based on many field tests conducted by the Ministry of Agriculture, Malaysia.

Pre-saturation is a significant initial phase before rice is planted. In this study, the water requirement was calculated in accordance with the recently recommended cropping irrigation schedule for the scheme, as reported by [39] and presented in Table 1. The schedule is designed for rice MR84, which is the widely adopted rice variety in Malaysia, with growth duration of 120–125 days. Wet direct seeding method is practiced in the irrigation scheme. Water for pre-saturation is allocated to the irrigation blocks of the four ISAs (each staggered by one month) at a rate of 18.5 mm/day/ha for a period of 14 days, followed by land preparation and drainage of excess water, if required.

2.8. Flow Analysis for Storage Pond

Because of the water shortage in the scheme, particularly during the dry season period, a storage pond was built along the main canal. Its main function is to store water during the period of low water demand in the scheme and release it in the period of high demand. The pond (reservoir) has an area of 88.41 ha with a storage pool area of 65 ha and pond water storage capacity of 1.5 million m^3 . The initial (critical) and full (maximum) storage were considered as 0.3 and 1.5 million m^3 , respectively. In order to analyze the reservoir release patterns in the study area, the following components were assessed: the daily supply into the storage pond, the release from the storage pond, the spill, and the total storage. The inflow into the reservoir is when the amount at the reservoir intake in the main canal is higher than the required amount downstream (at ISAs III and IV) and does not exceed maximum storage. Similarly, the release from the reservoir is when the amount at the reservoir intake in the main canal is less than the required amount downstream and the amount is not more than the critical storage.

Supply into the storage pond (Q_{isp}):

$$Q_{isp} = 0, \text{ for the first day}$$

For other days:

$$Q_{isp} = \begin{cases} Q_{mcR} - Q_{mc/ds}, & \text{if } Q_{mcR} > Q_{mc/ds}; (Q_{mcR} - Q_{mc/ds}) < (S_{fsp} - S_t) \\ 0, & \text{otherwise} \end{cases} \quad (16)$$

Release from the storage pond (Q_{rsp}):

$$Q_{rsp} = 0, \text{ for the first day}$$

$$Q_{rsp} = \begin{cases} S_t - S_{isp}, & \text{if } S_t > S_{isp}; (Q_{mc/ds} - Q_{mcR}) > (S_t - S_{isp}) \\ 0, & \text{otherwise} \end{cases} \quad (17)$$

$$Q_{osp} = 0, \text{ for the first day;}$$

For other days:

$$Q_{osp} = \begin{cases} (S_t + Q_{isp}) - S_{fsp}, & \text{if } S_t > S_{isp}; (Q_{mc}/ds - Q_{mcR}) > (S_t - S_{isp}) \\ 0, & \text{otherwise} \end{cases} \quad (18)$$

where Q_{mcR} is the available discharge at reservoir point along main canal; Q_{mc}/ds is the water demand at downstream from reservoir point along main canal; S_{fsp} is the full storage in the storage pond; S_t is the reservoir storage in the previous day; and S_{isp} is the critical storage in the storage pond. Finally, the total storage S_{t+1} in the reservoir at a given day is computed as:

$$S_{t+1} = S_t + Q_{isp} + ER - EP_{sp} - Q_{rsp} - Q_{osp} \quad (19)$$

EP_{sp} is the evaporation from the storage pond expressed as:

$$EP_{sp} = \frac{ET_o}{K_p} \quad (20)$$

where ER is the effective rainfall into the reservoir and K_p is the pan coefficient, 0.75.

2.9. Design and Development of Climate-Smart Agro-Hydrological Tool

The generated daily big data of about 700 GB was integrated using Excel-based Visual Basic for Applications (VBA), to visualize and analyze different irrigation and water parameters in the scheme under various management options for the historical (1976–2005) and future (2010–2099) periods. These parameters include various flows at SKC, BRH, TRH and at the key points along the main canal, water demand at different ISAs in the scheme, and reservoir releases/inflows and storage. Several programs based on ten GCMs under three RCP scenarios (RCP4.5, RCP6.0 and RCP8.5) were developed to design the interface. The graphical user interface is based on a mouse-driven pattern with pop-up windows, pull-down menus, and control buttons. The main interface of the model is linked with reference evapotranspiration and rainfall sub-modules. The former was designed using the FAO-56 Penman–Monteith model, to estimate daily ET_o (mm/day), while the latter was used to compute daily effective rainfall. The generated outputs from the two sub-modules can be imported directly to the main module. The tool, under different GCM and RCP realizations, is capable of visualizing and analyzing the integrated daily big data of all water resources, from the basin outlet upstream to the rice field downstream, through the flow within the rivers and the reservoir release/inflow/storage patterns.

To visualize and analyze any variable during the historical period, the name of the variable(s) and date are selected. For future periods, a realization of GCM and RCP scenarios must be selected from the list of the GCMs and RCPs 4.5, 6.0, and 8.5 before the selection of the date and variable(s) to be analyzed. The analysis could be for a single time segment (2010–2039, 2040–2069, or 2070–2099) or multiple periods, using a single GCM or multiple models. A maximum of four parameters can be visualized at one time. The visualization could be chosen in daily, weekly, monthly, seasonal, or longer time series and the results viewed in tabular and graphical forms. The developed climate-smart agro-hydrological tool was applied to Tanjung Karang Rice Irrigation Scheme Malaysia to assess climate change impacts on key agro-hydrological information. Numerous outputs from the model were obtained using both single GCM model(s) and multi-model projections. Nonetheless, due to space constraints, this paper only discusses a few selected outputs.

3. Results and Discussion

3.1. Hydrological Modeling

In both calibration and validation periods, the monthly observed and simulated discharges from the HEC-HMS model were compared. Results of R^2 , NSE, and PBIAS during the calibration and

validation periods were 0.74, 0.71, and 4.21, and 0.71, 0.69, and 5.32, respectively. These results indicate a satisfactory simulation, as the values are greater than 0.5 [40].

3.2. Hydraulic Modeling

To evaluate the hydraulic model, HEC-RAS daily observed and simulated discharge data from the model were compared. R^2 , NSE and PBIAS were 0.66, 0.64, and 0.94, and 0.65, 0.59, and 1.77, respectively, during calibration and validation periods. These show that the simulation is satisfactory since the values are greater than 0.5 [40]. However, the model compared to the calibration period underestimated some of the simulated discharge. Nevertheless, the model was able to optimally capture low and peak flows for most days.

3.3. Climate-Smart Agro-Hydrological Model Simulation Outputs

3.3.1. Hydro-Meteorological Variables

In the paddy water demand model, effective rainfall is an important factor for estimating the daily water requirements. Effective rainfall is a fraction of total rainfall received that can be used directly in the paddy field after losses due to runoff and deep percolation. To optimize the use of rainfall and save irrigation water for future usage, a reasonable estimation of future seasonal effective rainfall is therefore necessary. Changes in effective rainfall are substantially different with the GCM and RCP scenarios with no consistent pattern (Table 2). The Commonwealth Scientific and Industrial Research Organization (CSIRO) and Hadley Global Environment Model 2-Earth System (HadGEM2-ES) models show a substantial decrease in effective rainfall, while the Max Planck Institute-Earth System Model running on low resolution grid (MPI-ESM-LR) and Canadian Earth System Modelling (CANESM2) models forecast a notable increase. The change in effective rainfall, therefore, is not necessarily defined by the characteristics of a certain model, rather, it largely depends on its physical parameterization. These variations underline the inherent uncertainty of GCM forecasts on climate models. Analysis of simulated annual rainfall from different GCMs by [41] also found that each GCM exhibits a large spread of the annual rainfall. Predicting effective rainfall is thus a potential source of uncertainty in impact assessments. The model outputs reveal that future effective rainfall will decrease from the baseline period by an average of 9.39%, 34.33%, and 17.90% for RCP 4.5, RCP 6.0, and RCP 8.5, respectively, using the multiple models in the dry season period (Figure 3). There is a noticeable decrease of 38.47% (27.01%) in RCP 6.0 (RCP 8.5) in the latter part of the century (2080s) for the worst-case scenario (RCP 8.5). In Figure 3, the decrease is pronounced in March, April, May, and June. However, the season is wetter in April, May, and June during later future periods (2050s and 2080s). This indicates that future dry seasons might be wetter than the current dry season. This predicted rainfall might militate against the conditions of drought that currently often affect paddy schemes. In the wet season, effective rainfall is projected to respectively increase 3.46% (5.55%) for RCP 4.5 (RCP 8.5); for RCP 6.0 rainfall is expected to decrease (by 9.79%). However, in both seasons, the RCP6.0 scenario shows a different trend, projecting a higher rate of decrease in the dry season and an increase in the wet season in all future periods. This might be due to the lack of data available for this scenario in some GCM repositories (Table 2). Climate projections in the study location, therefore, show a decrease in the effective rainfall of the dry season (January–June) and an increase in the wet season (July–December). Based on these findings, flooding is likely to increase during the wet (main rice growing) season, as well as intermittent dry spells during the dry season. This difference in rainfall in both seasons needs to be taken into account in the scheme's water resource planning.

Table 2. Projected annual changes in effective rainfall (%) by global climate models (GCMs) under Representative Concentration Pathways (RCPs) 4.5, 6.0, and 8.5 for the periods 2010–2039, 2040–2069, and 2070–2099 relative to the 1976–2005 baseline period.

GCMs	RCP4.5			RCP6.0			RCP8.5		
	2020s	2050s	2080s	2020s	2050s	2080s	2020s	2050s	2080s
CANESM2	–	–	–	–	–	–	16.38	27.72	37.85
CCSM4	–0.98	3.86	3.95	–6.46	–2.97	0.59	–2.28	5.46	–3.65
CNRM	–6.58	–0.95	–4.47	–	–	–	–1.88	–7.05	0.00
CSIRO	–1.87	1.33	8.07	–4.65	–9.70	–7.14	0.29	–33.5	–72.20
GFDL-ESM2G	3.35	6.14	3.55	4.68	6.62	8.09	1.24	14.60	0.00
GFDL-ESM2M	5.56	2.92	6.47	7.23	14.46	14.16	11.72	5.15	9.28
HadGEM2-CC	13.75	–5.13	5.46	–	–	–	4.09	–1.47	0.14
HadGEM2-ES	1.97	–9.42	–0.65	–55.31	–55.46	–62.29	–0.78	–8.44	–8.23
MPI-ESM-LR	34.1	28.7	43.6	–	–	–	44.9	34.7	27.3
MRI-CGCM3	2.72	–2.88	10.14	–5.43	–0.16	–6.08	–3.17	3.85	–5.14

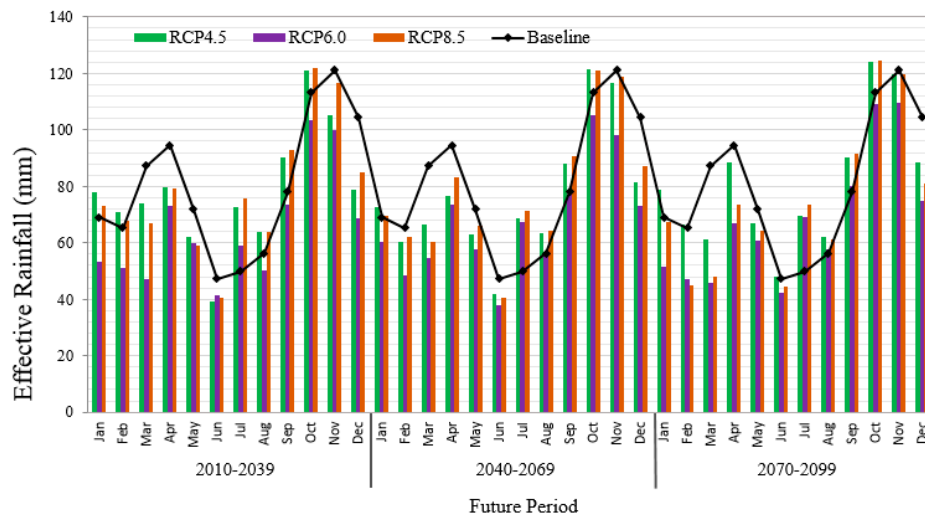


Figure 3. Projected average monthly effective rainfall using multiple models under RCPs 4.5, 6.0, and 8.5 for the periods 2010–2039, 2040–2069, and 2070–2099 with respect to the 1976–2005 baseline.

3.3.2. Temperature Projection

Temperature (maximum and minimum) has the greatest effect on the estimation of irrigation water demand [42]. The output of the model using multiple models indicates an increase in the future temperature (Table 3). The mean maximum temperature would increase by 1.18 °C, 1.14 °C, and 1.97 °C for RCPs 4.5, 6.0, and 8.5, respectively, compared to the baseline period (1976–2005). The model also reveals a noticeable increment (3.25 °C) from the most severe scenario (RCP8.5) in the latter part of the century (2080s). A similar change pattern is observed for the minimum temperature, however, with a higher rate. The projected temperature will assist in anticipating the condition of the basin for the purpose of future irrigation water demand planning, especially during the dry season months.

Although climate change impacts will vary due to differences in crop variety and local variations in growing seasons, crop management, etc., rising temperature and precipitation may escalate the deteriorating condition of the soil, which could have negative effects on rice production. Most crop yields will be negatively impacted by temperature rise and erratic rainfall, floods, and droughts [43]. According to [44], an increase in minimum temperature would be advantageous for rice production, however, higher increases in rainfall and mean temperature will negatively affect its production in the future. It is also noted that not all rice varieties could tolerate temperature rise while sustaining yields.

In addition, the standing crop failure due to prolonged submergence, flooding, and salinity should be addressed through the development of anticipatory adaptation strategies.

Our investigation of how climate change impacts irrigation water planning and management represents an attempt towards quantifying future changes in rice production. Consequently, a proper study of future changes in rice production for the scheme is necessary, as this was not covered in the present study because other yield-related data were not yet available.

Table 3. Projected changes in temperature under multi-model projections based on RCP scenarios relative to the baseline period of 1976–2005.

Period	Changes in Temperature under RCPs		
	RCP4.5	RCP6.0	RCP8.5
Maximum temperature (°C)			
2020s	0.68	0.52	0.82
2050s	1.29	1.06	1.85
2080s	1.57	1.85	3.25
Average	1.18	1.14	1.97
Minimum temperature (°C)			
2020s	0.71	0.62	0.92
2050s	1.36	1.16	1.95
2080s	1.75	1.85	3.36
Average	1.27	1.21	2.08

3.3.3. Impact on Potential Evapotranspiration

Potential evapotranspiration (ET_0) is a key element in computing and scheduling of irrigation requirements. Climate change affects all climatic parameters, including ET_0 . Values of ET_0 were computed based on downscaled meteorological variables using the FAO-56 Penman–Monteith method. The average maximum and minimum temperatures for the three scenarios of the RCP continue to rise during the 2020s, 2050s, and 2080s over the baseline period. In all GCM models, the probable rise in temperatures in each of the three emission scenarios is generally agreed. This means that in future, and particularly in dry season months, the scheme will be warmer. The findings of the Intergovernmental Panel on Climate Change (IPCC) for Southeast Asia show a similar pattern in the future [45]. According to RCPs 4.5, 6.0, and 8.5, the ET_0 will increase over the coming three periods by 1.6%–3.7%, 0.8%–4.7%, and 1.6%–9.1%, respectively. In the dry season (March–July), the monthly ET_0 rises are prominent (Figure 4). RCP 8.5 (most extreme) in the 2080s at 14.2% and RCP 6.0 at 0.2% are the most significant increases.

The study shows clearly that the expected increase in temperature directly impacts the irrigation requirements. Figure 5 indicates that there will be increased irrigation needs in the future. Climate-smart adaptation approaches are therefore crucial to meet demand for crop water under future climatic conditions.

The three possible RCP scenarios would theoretically result in a change in the monthly temperature according to the projection. RCP8.5 predicts a substantial increase in temperature every year with an average temperature of between 3.5 °C and 3.7 °C. More warming is expected over the wet season compared to the dry season in the irrigation system (Figure 6). Based on the GCM results, more water will be needed in future, except for the months of October and November. The reference evapotranspiration will rise in future periods as a result of the warming trends resulting from temperature increases.

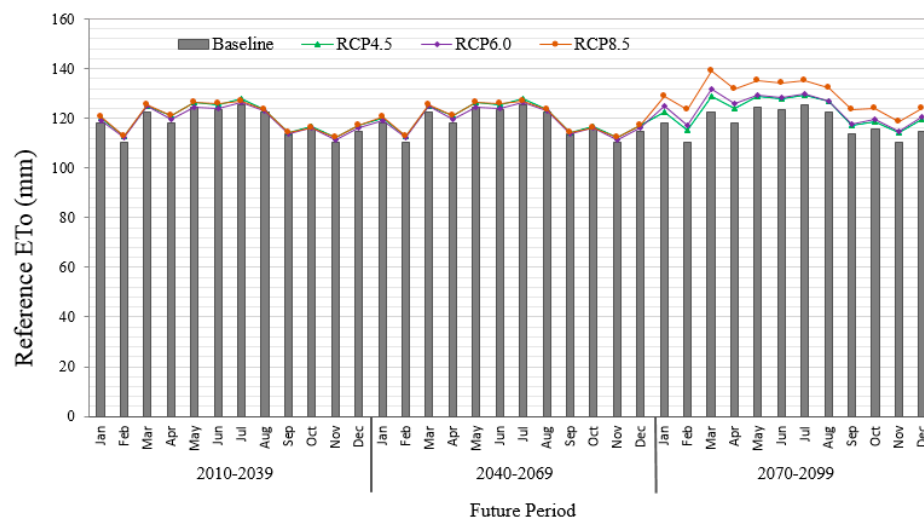


Figure 4. Projected mean monthly ensemble of multi-model reference evapotranspiration (ET_0) for RCP4.5, RCP6.0, and RCP8.5 scenarios and future periods of 2020s, 2050s, and 2080s compared to the baseline period.

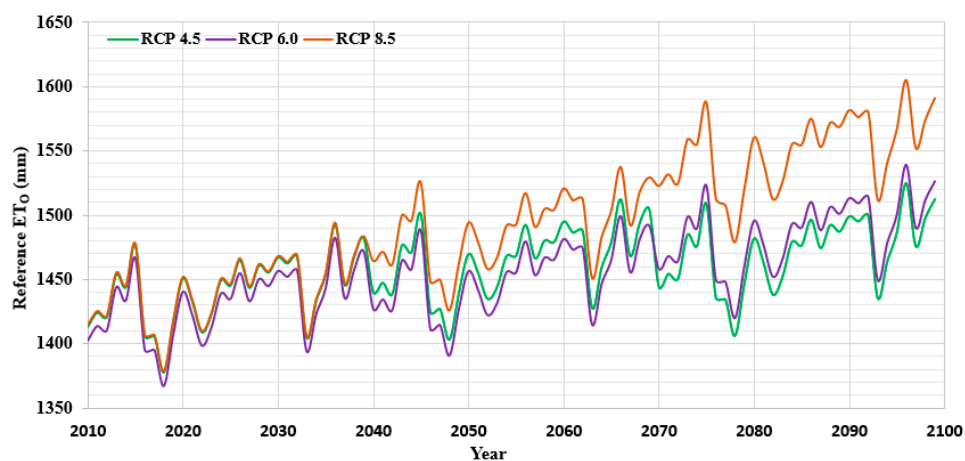


Figure 5. Projected multi-model annual reference evapotranspiration (ET_0) for the RCP4.5, RCP6.0, and RCP8.5 scenarios from 2010 to 2099.

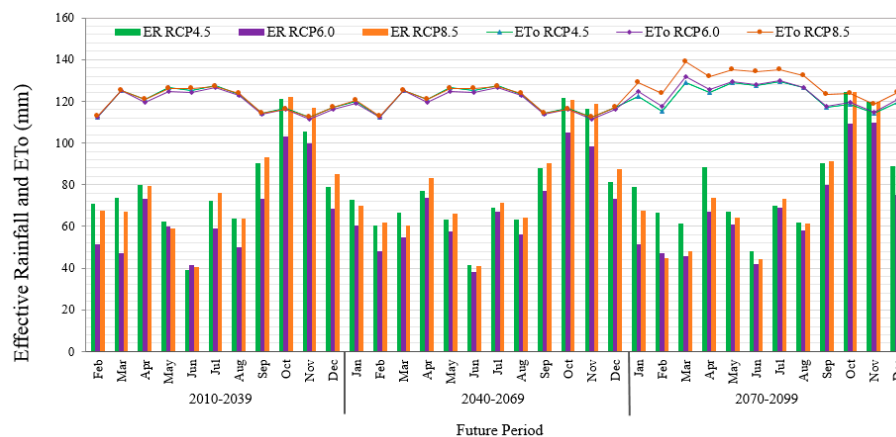


Figure 6. Projected monthly multi-model effective rainfall (ER) and reference evapotranspiration (ET_0) for RCP scenarios in future periods (2010–2099).

3.4. Modeling Streamflow under Climate Change Impacts

Figure 7 shows an example of average future changes in seasonal streamflow under multi-model projections based on RCP 4.5, 6.0, and 8.5 scenarios relative to the baseline period (1976–2005). The average changes for RCP 4.5, 6.0, and 8.5 are -0.40% , -1.68% , and -5.71% , respectively, during the dry season (Table 4). The model outputs suggest a decreasing pattern in streamflow in this season for all future periods, with a higher rate (-5.94%) expected under the RCP8.5 scenario in the latter part of the century (2080s). A similar change pattern is observed in the wet season, however, with a lower rate, except for RCP4.5, in which it is expected to increase (0.36%). The model output, therefore, highlights the changes in future streamflow at Bernam river basin to be more pronounced during the dry season period. This might be associated with the warmer temperature during this period, which consequently affects the future streamflow. The available water for supply to the scheme largely depends on the streamflow at the basin outlet. A significant change in the future streamflow translates to the available irrigation supply. Therefore, the scheme is predicted to experience water shortages, particularly during the dry season period. This would consequently affect the water resources in the scheme, which could lead to negative impacts on the overall crop production in the area. A similar decrease in annual streamflow was observed by [4] and [5]. Although the changes in streamflow are not great, the basin may suffer from reduced water pressure, particularly during the dry season period.

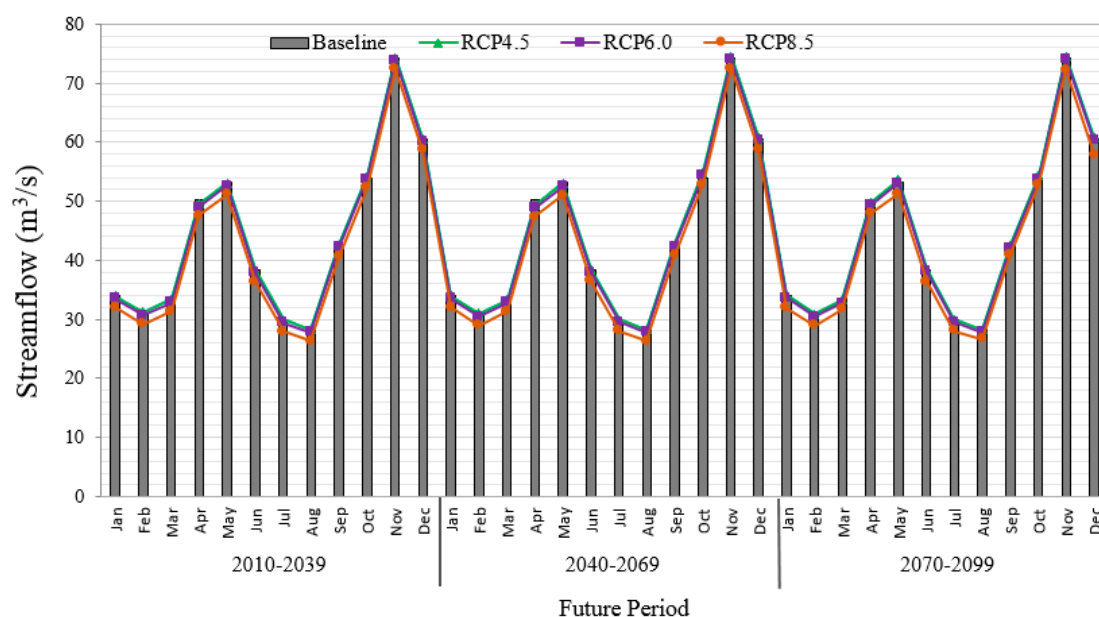


Figure 7. Projected mean monthly streamflow from multiple models for three RCP scenarios (RCPs 4.5, 6.0, and 8.5) for three future periods of 2010–2039, 2040–2069, and 2070–2099 relative to the baseline period of 1976–2005.

Projection of Available Supply for Irrigation

The projected available water for supply to the scheme, which largely depends on the streamflow from the Bernam basin, would decrease in both dry and main seasons in all future periods, with a noticeable decrease (-12.57%) in the latter part of the century (2080s) for RCP 8.5 during the dry season (Figure 8). The average changes for RCP4.5, 6.0, and 8.5 are -7.94% (-7.86%), -10.30% (-9.84%), and -12.42% (-12.26%) during the dry (and main) seasons, respectively. The model outputs reveal that the decrease in available water for supply would be higher during the dry season period. This might be due to the decrease in rainfall and warmer temperatures during the season, which increase the rate of evapotranspiration more compared to the wet season period, and consequently affect the future available supply. Therefore, the model could be integrated with adaptive cropping patterns to enhance future water allocation. Since the project is a run-of-the-river project, a recommended supply could be

adopted that enables proportionate distribution of water among the tertiary canals through proper control of the off-take structure gate. A factor can be introduced (considering the rice's water-sensitive growth stages) to achieve an equitable supply. The factor depends on the management and operational decisions in the command area with respect to the available water for irrigation. With the advance of the irrigation season, the recommended irrigation supply (allowable supply based on available water) for tertiary canals is proposed.

Table 4. Projected changes in streamflow under multi-model projections based on RCP scenarios relative to the baseline period of 1976–2005.

Irrigation Season	Period	Changes (%) in Streamflow		
		RCP4.5	RCP6.0	RCP8.5
Dry Season	2020s	−0.40	−1.70	−5.66
	2050s	−0.63	−1.90	−5.54
	2080s	−0.18	−1.44	−5.94
	Average	−0.40	−1.68	−5.71
Wet Season	2020s	0.19	−0.84	−3.92
	2050s	0.59	−0.47	−3.67
	2080s	0.31	−0.71	−3.90
	Average	0.36	−0.67	−3.83

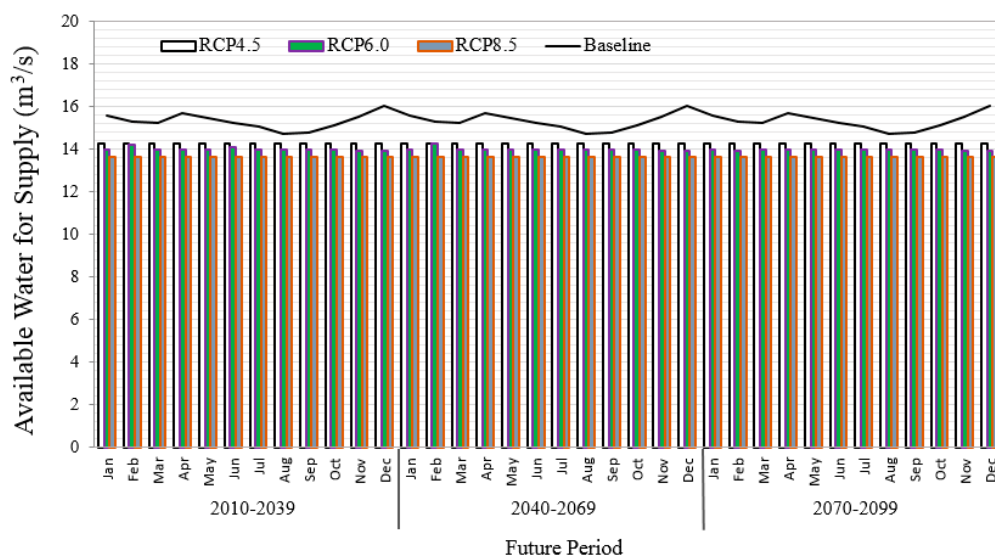


Figure 8. Projected mean monthly available supply from multiple models for three RCP scenarios (RCPs 4.5, 6.0, and 8.5) for three future periods of 2010–2039, 2040–2069, and 2070–2099 relative to the baseline period of 1976–2005.

3.5. Water Demand Projection

The projected water demand during the dry season under multi-model projections based on RCP4.5, 6.0, and 8.5 scenarios suggests an increasing pattern in water demand, with a higher increase (11.09%) expected under the RCP8.5 scenario in the latter part of the century (2080s), except for RCP6.0, under which a decreased pattern is predicted in some years (Table 5 and Figure 9). The average changes in this season are 5.59%, −5.75%, and 10.71% for RCPs 4.5, 6.0, and 8.5, respectively. The model outputs reveal that the water demand increment in the dry season is due to the increase in temperature and decrease in rainfall during the season. During the wet season, water demand is projected to decrease 2.6% (6.2%) in all three future periods for RCP 4.5 (RCP 8.5) scenarios. However, RCP 6.0 predicts an increase of about 9.0% in the same season. Although temperature is projected to increase in the

wet season, the reason for the decrease in the water demand in the season, as revealed by the model, is due to a significant contribution from the effective rainfall following the Northeast Monsoon rainfall during the wet season, which compensates for the warmer periods. Tukimat et al. [46] also reported that climate change may not significantly affect water availability in the countries of South-East Asia because water demand will decrease due to increased rainfall. However, in both seasons the RCP6.0 scenario shows different change patterns. This might be due to the lack of data available for this scenario in some GCM repositories (Table 2). Therefore, the RCP 6.0 scenario should only be used with extreme care in the future implementation of the developed model.

Table 5. Projected annual changes in water demand under multi-model projections based on RCP scenarios.

Irrigation Season	Period	Annual Changes (%) in Water Demand under RCPs		
		RCP4.5	RCP6.0	RCP8.5
Dry Season	2020s	4.36	5.54	10.03
	2050s	6.21	−11.40	11.02
	2080s	6.21	−11.40	11.09
	Average	5.59	−5.75	10.71
Wet Season	2020s	−2.3	−4.5	−5.4
	2050s	−2.4	17.5	−5.9
	2080s	−3.3	14.0	−7.3
	Average	−2.6	9.0	−6.2

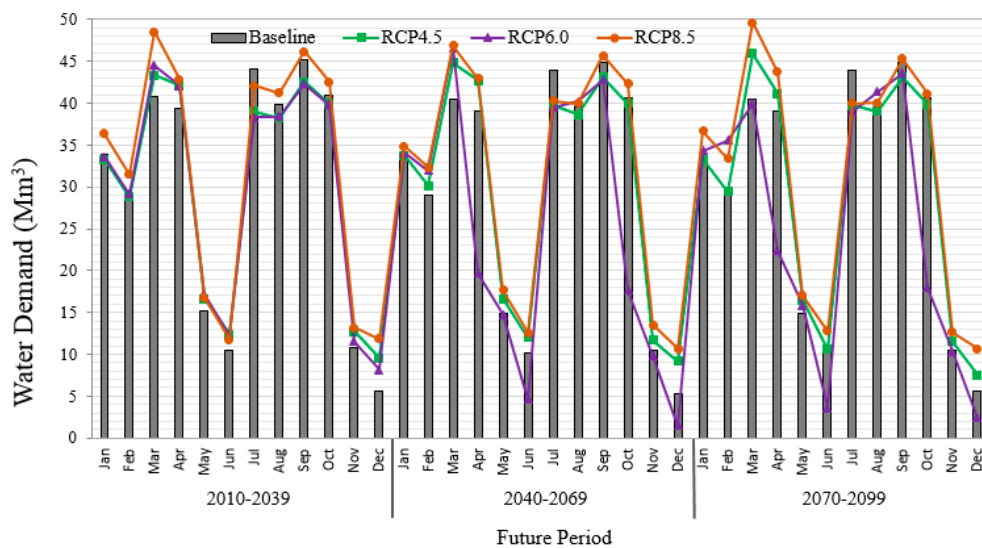


Figure 9. Projected mean monthly water demand from multiple models for three RCP scenarios (RCPs 4.5, 6.0, and 8.5) for three future periods of 2010–2039, 2040–2069, and 2070–2099 relative to the baseline period of 1976–2005.

The model outputs also indicate the scheme will require more irrigation water in the future (with a higher rate under RCP8.5) in the months of March and September during dry and wet seasons, respectively. This is because in March (during the dry season), ISA III requires pre-saturation plus normal irrigations for ISAs I, II, and III, which require larger irrigation amounts. In addition, in September (during the wet season), ISA III is pre-saturated together with ISAs I, II, and III under normal irrigations. On the other hand, less water demand is observed from May to June in the dry season period and from November to December in the wet season. Normal irrigations are only observed in these periods, which require lesser irrigation amount. The water demand in the scheme will differ greatly over the months of the dry season in the future, and the increase in effective rainfall

during the wet season will compensate for the high dry season water demand. No irrigation will therefore be needed in the months of May and June. The main challenge, however, will be to properly manage the monthly variation of irrigation water demand in the command area. Failure to correctly manage the irrigation system will lead to much greater uncertainty as the project is a run-of-the-river irrigation scheme with limited storage facility.

The anticipated irrigation demands of the rice crop and the expected available water for supply to the scheme were examined for the future emission scenarios. Figure 10, based on the model outputs using multiple models, demonstrates that the water supply to the scheme is not regulated based on the water demand. Irrigation supply is thus observed to fluctuate during the seasons with over-supply in some periods and under-supply in others. An over-supply occurs when the ratio of available water for supply to the water demand is greater than 1, and under-supply is considered if the ratio is less than unity. A balance between water supply and demand is attained when the ratio is 1. The model outputs reveal that, in future, the scheme would be over-supplied in January–February and May–June during the dry season period, and November–December during the wet season, with notable excess supplies in June and December (Table 6). However, during March–April in the dry season and July–October (except October in the 2050s and 2080s for RCP 6.0) in the wet season, a supply shortage is projected based on the irrigation demand for RCPs 4.5, 6.0, and 8.5. Since the project is a run-of-the-river project, a reservoir to store more water for future use based on the modeled discharge at the supply intake would be useful. For effective irrigation water management, a good balance between water supply and demand needs to be achieved. This could be attained through operational actions, many of which require predictive models and instruments to be applied [47]. Therefore, the developed model could be integrated with adaptive cropping patterns to enhance the water allocation through the proper supply of the needed water in the scheme, thereby avoiding over-supply in the period of low demand and under-supply in the period of high demand.

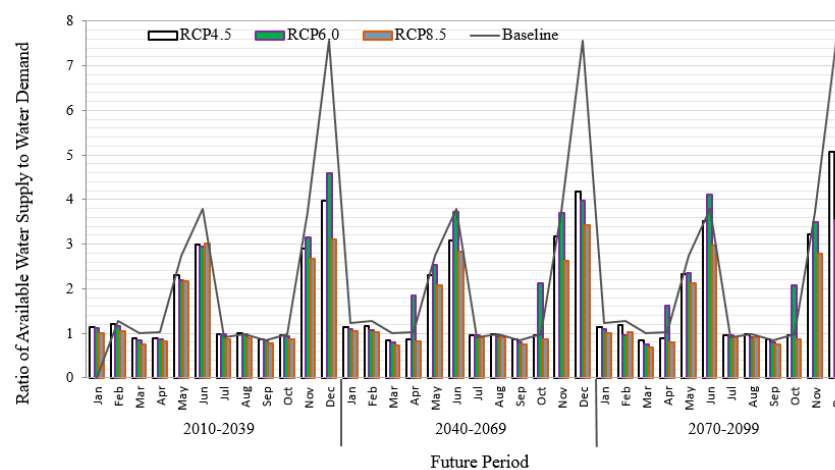


Figure 10. Projected ratio of available water for supply (WS) to water demand (WD) from multiple models for three RCP scenarios (RCPs 4.5, 6.0, and 8.5) for three future periods of 2010–2039, 2040–2069, and 2070–2099 relative to the baseline period of 1976–2005.

Table 6. Historical and projected water supply excess/shortage under RCP scenarios 4.5, 6.0, and 8.5 for the periods 2010–2039, 2040–2069, and 2070–2099.

Season	Historical	RCP4.5			RCP6.0			RCP8.5		
	1976–2005	2020s	2050s	2080s	2020s	2050s	2080s	2020s	2050s	2080s
Dry season										
Jan	2.92	1.80	1.65	1.78	1.38	1.26	1.16	0.11	0.67	−0.11
Feb	3.35	2.46	1.92	2.19	2.01	0.89	−0.61	0.76	0.42	0.20
Mar	−0.03	−1.94	−2.47	−2.87	−2.66	−3.50	−4.61	−4.46	−4.94	−6.52
Apr	0.51	−1.98	−2.23	−1.61	−2.27	6.38	5.33	−2.87	−2.90	−3.53
May	9.84	8.06	8.07	8.14	7.56	8.44	8.04	7.37	7.10	7.22
June	11.21	9.50	9.65	10.20	9.23	12.22	12.57	9.12	8.83	9.07
Wet season										
Jul	−1.40	−0.34	−0.62	−0.59	−0.32	−0.76	−0.61	−2.03	−1.40	−1.23
Aug	−0.13	−0.02	−0.15	−0.30	−0.37	−1.03	−1.49	−1.73	−1.26	−1.23
Sep	−2.63	−2.22	−2.36	−2.36	−2.38	−3.62	−3.56	−4.22	−4.39	−4.73
Oct	−0.15	−0.68	−0.67	−0.62	−0.90	7.37	7.25	−2.23	−2.16	−2.08
Nov	11.39	9.34	9.76	9.81	9.51	10.17	9.97	8.56	8.45	8.77
Dec	13.90	10.68	10.84	11.45	10.92	13.44	13.02	9.25	9.67	9.69

Note: water supply > water demand (excess, +), water supply < water demand (shortage, −).

4. Conclusions

A user-friendly agro-hydrological model was developed and successfully deployed for adaptive irrigation and wise water resource management towards water security in Tanjung Karang Rice Irrigation Scheme in Malaysia under new climate change realities. The model outputs reveal that future effective rainfall will decrease from the baseline period in the dry season and increase in the wet season. The decrease is more pronounced in March, April, May, and June. However, the season becomes wetter in April, May, and June during the later future periods (2050s and 2080s) compared to the 2020s, which indicates that future dry seasons might be wetter than the current dry season. This predicted rainfall might militate against the conditions of drought that currently impact the paddy scheme. Based on these findings, flooding is likely to increase during the wet (main rice growing) season, as well as intermittent dry spells during the dry season. This difference in rainfall in both seasons needs to be taken into account in the scheme's water resource planning.

The projected available water for supply to the scheme, which largely depends on the streamflow from the Bernam basin, would decrease in both dry and wet seasons, with a notable decrease during the dry season period. Simulated flows from the developed model could be integrated with adaptive cropping patterns to enhance future water allocation. Since the project is a run-of-the-river project, a recommended supply could be adopted that enables proportionate distribution of water among the tertiary canals through proper control of the off-take structure gate. The water demand in the scheme will differ greatly during the months of the future dry seasons, with the increase in effective rainfall during the wet season compensating for the high dry season water demand. No irrigation will therefore be needed in the months of May and June. The main challenge, however, will be to properly manage the monthly variation of irrigation water demand in the command area. Failure to effectively manage the irrigation system will lead to much greater uncertainty as the project is a run-of-the-river irrigation scheme with limited storage facility. The model can be extended by taking into account the historical data of local stations, the GCMs, and features of the irrigation scheme, even though it is customized for local application to the Tanjung Karang Rice Irrigation Scheme.

Based on the study findings, the following potential implications can be drawn from the model outputs with suggested options:

- (1) Occurrence of floods and droughts: Due to increased rainfall events, the future of paddy farming is likely to face floods during the wet season and droughts during the dry season. Such changes

will influence planning for the scheme's water resources. Hence, vigilance will be needed to ensure proper management of the rice crop to reduce negative impacts.

- (2) Construction of storage reservoirs: While shortages of water will be experienced in some periods during the season, there will be an excess of water in other periods, which would run as waste. A storage reservoir was recently built in the scheme, however, its capacity is inadequate. Alternatively, reservoir(s) to store more water for future use based on the modeled discharge at the supply intake would be useful. The excess water could be stored in the reservoir(s) and used during the periods of high demand.
- (3) Altering of the paddy cropping schedule: In general, the issue of climate change may not impose significant water shortages for paddy cultivation in terms of physical water shortages. However, water-use efficiency could be improved with an additional cropping season (i.e., five seasons per two-year period), considering the projected increase in rain water. This could be achieved by improvements in crop patterns and alternate approaches in water management.

Author Contributions: Conceptualization, H.I. and M.R.K.; Data curation, M.S.F.b.M.; Formal analysis, H.I. and A.F.b.A.; Funding acquisition, M.R.K.; Investigation, A.F.b.A.; Methodology, H.I. and M.R.K.; Project administration, M.R.K. and A.F.b.A.; software, H.I.; supervision, M.R.K.; Validation, H.I.; Visualization, A.F.b.A.; Writing—original draft, H.I. and M.S.F.b.M.; Writing—review & editing, M.R.K. and A.F.b.A. All authors have read and agreed to the published version of the manuscript.

Funding: This research was funded by UNIVERSITI PUTRA MALAYSIA, Putra Grant No: 9678600 and the MINISTRY OF HIGHER EDUCATION, FRGS Grant No: FRGS/1/2019/WAB01/UPM/02/37.

Acknowledgments: The authors wish to acknowledge Department of Irrigation and Drainage, Malaysia and National Hydraulic Research Institute of Malaysia (NAHRIM) for providing hydro-meteorological data.

Conflicts of Interest: The authors declare no conflict of interest.

References

1. Haghighi, A.T.; Darabi, H.; Shahedi, K.; Solaimani, K.; Kløve, B. A scenario-based approach for assessing the hydrological impacts of land use and climate change in the Marboreh Watershed, Iran. *Environ. Model. Assess.* **2020**, *25*, 41–57. [\[CrossRef\]](#)
2. United Nations Water Home Page. Available online: <https://www.unwater.org/publications/climate-change-adaptation-pivotal-role-water/> (accessed on 19 February 2019).
3. Haro-Montegudo, D.; Palazón, L.; Beguería, S. Long-term Sustainability of Large Water Resource Systems under Climate Change: A Cascade Modeling Approach. *J. Hydrol.* **2020**, *582*, 124546. [\[CrossRef\]](#)
4. Arnell, N.; Reynard, N. The effects of climate change due to global warming on river flows in Great Britain. *J. Hydrol.* **1996**, *183*, 397–424. [\[CrossRef\]](#)
5. Chien, H.; Yeh, P.J.F.; Knouft, J.H. Modeling the potential impacts of climate change on streamflow in agricultural watersheds of the Midwestern United States. *J. Hydrol.* **2013**, *491*, 73–88. [\[CrossRef\]](#)
6. Dlamini, N.S. Decision Support System for Water Allocation in Rice Irrigation Scheme under Climate Change Scenarios. Ph.D. Thesis, Universiti Putra Malaysia, Seri Kembangan, Malaysia, 2017.
7. Ma, Z.; Kang, S.; Zhang, L.; Tong, L.; Su, X. Analysis of impacts of climate variability and human activity on streamflow for a river basin in arid region of northwest China. *J. Hydrol.* **2008**, *352*, 239–249. [\[CrossRef\]](#)
8. CGSpace Home Page. Available online: <https://cgspace.cgiar.org/handle/10568/107279> (accessed on 19 February 2019).
9. Ghosh, M. Climate-smart Agriculture, Productivity and Food Security in India. *J. Dev. Policy Pract.* **2019**, *4*, 166–187. [\[CrossRef\]](#)
10. Ding, Y.; Wang, W.; Song, R.; Shao, Q.; Jiao, X.; Xing, W. Modeling spatial and temporal variability of the impact of climate change on rice irrigation water requirements in the middle and lower reaches of the Yangtze River, China. *Agric. Water Manag.* **2017**, *193*, 89–101. [\[CrossRef\]](#)
11. Flörke, M.; Schneider, C.; McDonald, R.I. Water competition between cities and agriculture driven by climate change and urban growth. *Nat. Sustain.* **2018**, *1*, 51. [\[CrossRef\]](#)
12. Xu, X.; Jiang, Y.; Liu, M.; Huang, Q.; Huang, G. Modeling and assessing agro-hydrological processes and irrigation water saving in the middle Heihe River basin. *Agric. Water Manag.* **2019**, *211*, 152–164. [\[CrossRef\]](#)

13. Chandrasiri, S.; Galagedara, L.; Mowjood, M. Impacts of rainfall variability on paddy production: A case from Bayawa minor irrigation tank in Sri Lanka. *Paddy Water Environ.* **2020**, *18*, 1–12. [[CrossRef](#)]
14. Nguyen, Q.D.; Roussey, C.; Poveda-Villalón, M.; Vaulx, C.D.; Chanet, J.P. Development experience of a Context-Aware System for Smart Irrigation Using CASO and IRRIG Ontologies. *Appl. Sci.* **2020**, *10*, 18033. [[CrossRef](#)]
15. Rowshon, M.; Dlamini, N.; Mojid, M.; Adib, M.; Amin, M.; Lai, S. Modeling climate-smart decision support system (CSDSS) for analyzing water demand of a large-scale rice irrigation scheme. *Agric. Water Manag.* **2019**, *216*, 138–152. [[CrossRef](#)]
16. Wanhyun, C.; Myung, H.N.; Yuha, P.; Deok, H.K.; Yongbeen, C. Prediction of Weights during Growth Stages of Onion Using Agricultural Data Analysis Method. *Appl. Sci.* **2020**, *10*, 2094. [[CrossRef](#)]
17. Ghobadi, M.; Ebrahimian, H.; Abbasi, F.; Norouzi, S. Development and application of a seasonal furrow irrigation model (SFIM). *J. Irrig. Drain.* **2020**, *69*, 1–191.
18. Jiang, J.; Feng, S.; Ma, J.; Huo, Z.; Zhang, C. Optimizing regional irrigation water use by integrating a two-level optimization model and an agro-hydrological model. *Agric. Water Manag.* **2016**, *178*, 76–88. [[CrossRef](#)]
19. Noory, H.; Van Der Zee, S.; Liaghat, A.M.; Parsinejad, M.; Van Dam, J. Distributed agro-hydrological modeling with SWAP to improve water and salt management of the Voshmgir Irrigation and Drainage Network in Northern Iran. *Agric. Water Manag.* **2011**, *98*, 1062–1070. [[CrossRef](#)]
20. Ma, Y.; Feng, S.; Huo, Z.; Song, X. Application of the SWAP model to simulate the field water cycle under deficit irrigation in Beijing, China. *Math. Comput. Model.* **2011**, *54*, 1044–1052. [[CrossRef](#)]
21. Jiang, J.; Feng, S.; Ma, J.; Huo, Z.; Zhang, C. Irrigation management for spring maize grown on saline soil based on SWAP model. *Field Crops Res.* **2016**, *196*, 85–97. [[CrossRef](#)]
22. Van Gaalen, H.; Vanuytrecht, E.; Willems, P.; Diels, J.; Raes, D. Bridging rigorous assessment of water availability from field to catchment scale with a parsimonious agro-hydrological model. *Environ. Model. Assess.* **2017**, *94*, 140–156. [[CrossRef](#)]
23. Siad, S.M.; Iacobellis, V.; Zdruli, P.; Gioia, A.; Stavi, I.; Hoogenboom, G. A review of coupled hydrologic and crop growth models. *Agric. Water Manag.* **2019**, *224*, 105746. [[CrossRef](#)]
24. Amin, M.; Rowshon, M.; Aimrun, W. Paddy water management for precision farming of rice. *Curr. Issues Water Manag.* **2011**, *6*, 107–142.
25. DID and JICA, Detailed study of water resources availability Northwest Selangor Integrated Agricultural Development Project. In *Final Report*; JICA: Tokyo, Japan, 1996; Volume 1.
26. Rowshon, M.; Mojid, M.; Amin, M.; Azwan, M.; Yazid, A. Improving irrigation water delivery performance of a large-scale rice irrigation scheme. *J. Irrig. Drain. E-Asce.* **2014**, *140*, 04014027. [[CrossRef](#)]
27. Ghosh, S.; Mujumdar, P. Nonparametric methods for modeling GCM and scenario uncertainty in drought assessment. *Water Resour. Res.* **2007**, *43*, W07405. [[CrossRef](#)]
28. New, M.; Hulme, M. Representing uncertainty in climate change scenarios: A Monte-Carlo approach. *Integr. Assess.* **2000**, *1*, 203–213. [[CrossRef](#)]
29. Abatzoglou, J.T.; Brown, T.J. A comparison of statistical downscaling methods suited for wildfire applications. *Int. J. Climatol.* **2012**, *32*, 772–780. [[CrossRef](#)]
30. Fang, G.; Yang, J.; Chen, Y.; Zammit, C. Comparing bias correction methods in downscaling meteorological variables for a hydrologic impact study in an arid area in China. *Hydrol. Earth Syst. Sci.* **2015**, *19*, 2547–2559. [[CrossRef](#)]
31. Wong, C.; Venneker, R.; Jamil, A.; Uhlenbrook, S. Development of a gridded daily hydrometeorological data set for Peninsular Malaysia. *Hydrol. Process.* **2011**, *25*, 1009–1020. [[CrossRef](#)]
32. Wong, C.; Venneker, R.; Uhlenbrook, S.; Jamil, A.; Zhou, Y. Variability of rainfall in Peninsular Malaysia. *Hydrol. Earth Syst. Sci. Discuss.* **2009**, *6*, 5471–5503. [[CrossRef](#)]
33. Meenu, R.; Rehana, S.; Mujumdar, P. Assessment of hydrologic impacts of climate change in Tungabhadra river basin, India with HEC-HMS and SDSM. *Hydrol. Process.* **2013**, *27*, 1572–1589. [[CrossRef](#)]
34. Babel, B.S.P.; Walid, S.M. Climate change and water resources in the Bagmati River, Nepal. *Theor. Appl. Climatol.* **2014**, *115*, 639–654. [[CrossRef](#)]
35. USACE-HEC. Hydraulic Reference Manual. In *US Army Corps of Engineers*; USACE-HEC: Davis, CA, USA, 2016.
36. Chow, V.T. *Open Channel Hydraulics*; McGraw-Hill Book Company: New York, NY, USA, 1959.

37. Chan, C.; Cheong, A. Seasonal weather effects on crop evapotranspiration and rice yield. *J. Trop. Agric. Food Sci.* **2001**, *29*, 77–92.
38. Allen, R.G.; Pereira, L.S.; Raes, D.; Smith, M. Crop evapotranspiration-Guidelines for computing crop water requirements-FAO Irrigation and drainage paper 56. *Fao Rome* **1998**, *300*, D05109.
39. IADA. *Final Report: Kajian Keberkesanan Talianir Tersier Di Seluruh Kawasan IADA Barat Laut Selangor*; Paradigm Ingenieurs SDN BHD: Selangor Darul-Ehsan, Malaysia, 2018.
40. Moriasi, D.N.; Arnold, J.G.; Van Liew, M.W.; Bingner, R.L.; Harmel, R.D.; Veith, T.L. Model evaluation guidelines for systematic quantification of accuracy in watershed simulations. *Trans. ASABE* **2007**, *50*, 885–900. [[CrossRef](#)]
41. Dlamini, N.; Rowshon, M.; Saha, U.; Lai, S.; Fikri, A.Z.; Zubaidi, J. Simulation of future daily rainfall scenario using stochastic rainfall generator for a rice-growing irrigation scheme in Malaysia. *Asian J. Appl. Sci.* **2015**, *3*, 492–506.
42. Goodarzi, M.; Eslamian, S. Performance evaluation of linear and nonlinear models for the estimation of reference evapotranspiration. *Int. J. Hydrol. Sci. Technol.* **2018**, *8*, 1–15. [[CrossRef](#)]
43. Soltani, A.A.F.; Zeynali, E.; Galeshi, S.A.; Niari, N. Simulating GFDL predicted climate change impacts on rice cropping in Iran. *J. Agric. Sci.* **2001**, *3*, 81–90.
44. Shakoor, U.; Saboor, A.; Baig, I.; Afzal, A.; Rahman, A. Climate variability impacts on rice crop production in Pakistan. *Pak. J. Agric. Sci.* **2015**, *28*, 19–27.
45. McKague, K.; Rudra, R.; Ogilvie, J. ClimGen-a convenient weather generation tool for Canadian climate stations. In Proceedings of the Meeting of the CSAE/SCGR Canadian Society for Engineering in Agricultural Food and Biological Systems, Montreal, QC, Canada, 6–9 July 2003.
46. Tukimat, N.; Harun, S.; Shahid, S. Modeling irrigation water demand in a tropical paddy cultivated area in the context of climate change. *J. Water Res. Plan Manage.* **2017**, *143*, 05017003. [[CrossRef](#)]
47. De Souza Groppo, G.; Costa, M.A.; Libânio, M. Predicting water demand: A review of the methods employed and future possibilities. *Water Supply* **2019**, *19*, 2179–2198. [[CrossRef](#)]



© 2020 by the authors. Licensee MDPI, Basel, Switzerland. This article is an open access article distributed under the terms and conditions of the Creative Commons Attribution (CC BY) license (<http://creativecommons.org/licenses/by/4.0/>).